Research in Pharmaceutical Sciences, October 2025; 20(5): 635-650
Received: 21-02-2025
Peer Reviewed: 09-05-2025
Revised: 27-05-2025
Accepted: 23-07-2025
Published: 20-10-2025

School of Pharmacy & Pharmaceutical Sciences
Isfahan University of Medical Sciences

Review Article

Exploring cell dynamics and tumor microenvironments: a comprehensive review of decellularized extracellular matrix (dECM) scaffolds in breast and prostate cancer research

Sho'leh Ghaedamini[1,2], Forouzan Rahmani[2], Zahra Sadeghi[1], Maryam Anjomshoa[2], and Ali Honarvar[3,*]

[1]*Department of Anatomical Sciences, School of Medicine, Isfahan University of Medical Sciences, Isfahan, Iran.*
[2]*Department of Anatomical Sciences, Faculty of Medicine, Shahrekord University of Medical Sciences, Shahrekord, Iran.*
[3]*Cellular and Molecular Research Center, Faculty of Medicine, Yasuj University of Medical Sciences, Yasuj, Iran.*

Abstract

Background and Purpose: Decellularized extracellular matrix (dECM) scaffolds offer advanced platforms for studying breast and prostate cancer, enabling the replication of the tumor microenvironment (TME) with high fidelity. This review summarizes methodologies for creating dECM scaffolds, highlighting their biochemical and mechanical properties that enable up to 70% greater physiological relevance compared to traditional two-dimensional cultures.

Search Strategy: A systematic literature search was conducted on PubMed, Scopus, and Web of Science databases (2010-2025) using keywords such as "decellularized extracellular matrix," "breast cancer," "prostate cancer," and "tumor microenvironment." Inclusion criteria focused on peer-reviewed studies employing dECM scaffolds in breast and prostate cancer research.

Findings: Key findings reveal that dECM scaffolds effectively mimic tissue-specific TMEs, facilitating the study of tumor-stroma interactions, cellular responses, and drug resistance in breast and prostate cancers. dECM supports enhanced understanding of cancer progression mechanisms, including increased invasiveness, chemoresistance, and cell proliferation. Differences in decellularization methods influence ECM composition and scaffold function. Challenges, including standardization, clinical validation, and scalability, remain.

Conclusion and Future Trends: dECM scaffolds hold great potential to advance cancer biology research and precision therapy development by providing biomimetic platforms. Future directions include integrating bioengineering advancements, AI-assisted ECM analysis, organoid and organ-on-chip models, and enhanced decellularization protocols to improve model fidelity and clinical relevance.

Keywords: *Breast cancer; Decellularization; Extracellular matrix; Prostate cancer; Scaffold.*

Table of Contents

*Corresponding author: A. Honarvar
Tel: +98-7433230290, Fax: +98-7433235153
Email: honarvarali14@gmail.com

Access this article online

Website: http://rps.mui.ac.ir

DOI: 10.4103/RPS.RPS_26_25

1. INTRODUCTION

Cancer is a leading global cause of mortality, with rising incidence rates driving the need for advanced research models (1). Among cancers, breast cancer (BC) and prostate cancer (PCa) are the most prevalent malignancies in women and men, respectively, selected for their high metastatic potential and complex stromal interactions that challenge treatment outcomes (2-4). The extracellular matrix (ECM), a critical component of the tumor microenvironment (TME), undergoes remodeling in cancer, where tumor and stromal cells alter collagen and fibronectin deposition, degradation, and crosslinking, creating a stiffer TME (5). These ECM changes promote clinical challenges, enhancing metastasis through invasion and migration, and conferring therapy resistance by shielding cancer cells from drugs and immune responses (6). Traditional two-dimensional (2D) cell cultures and synthetic scaffolds fail to replicate the TME's three-dimensional (3D) architecture and biochemical cues, limiting their utility in modeling tumor dynamics and drug responses (7,8). Decellularized ECM (dECM) scaffolds overcome these limitations by preserving native ECM composition, mechanical properties, and tissue-specific signals, offering a superior platform for BC and PCa research (9). This review leverages dECM to elucidate TME-driven mechanisms in BC and PCa, aiming to inform the development of targeted therapeutic strategies.

1.1. dECM scaffold

dECM scaffolds, widely used in tissue engineering, are generated by removing cellular components while preserving the 3D structure and protein content of the ECM (9-11). These scaffolds replicate tissue-specific ECM composition, providing biochemical signals for cell-ECM interactions that drive cancer cell behavior and metastasis. By mimicking *in vivo* environments, dECM models enhance studies of tumor growth, anticancer therapy efficacy, and drug resistance (12-14). Decellularized matrices derived from animal models, patient samples, and cell cultures enable the investigation of the complete range of matrix components found in native tissues (15).

Patient-derived dECM scaffolds replicate the TME in breast and prostate cancer, enabling personalized drug response predictions by mimicking ECM composition and stiffness. These scaffolds, when seeded with patient cells, reflect tumor behaviors like epithelial-mesenchymal transition (EMT) and chemoresistance, with proteomic analyses identifying biomarkers and co-cultures predicting immunotherapy outcomes (11,16-19). However, ECM variability and low biopsy yields challenge standardization and scalability for high-throughput drug screening (11,20). Advanced decellularization and bioengineering, along with rigorous quality control to meet regulatory standards, are essential to ensure reproducibility and clinical translation (9,21).

Recent studies demonstrate that decellularized tumor-derived ECM enhances tumorigenic activity by modulating tumor cell behavior (20). Colon cancer spheroids cultured on ECM from human liver metastases exhibit faster growth than those on healthy colon-derived ECM (22). Similarly, glioblastoma cells cultured on patient-derived decellularized tumor matrix display altered morphology and enhanced migration compared to collagen gels (23).

1.2. Comparison of Sources for dECM

Two primary sources of dECM exist: native tissues and organs of the organism, and regenerated tissues and organs derived from cultured cells (16,24). Decellularization techniques are critical in preparing dECM for cancer research, as they significantly influence its composition and structure, thereby affecting cellular behavior (7). In tumor modeling, *in vitro* decellularized models provide sophisticated, accessible, and biologically relevant scaffold-based systems (11).

1.3. Comparison of decellularization methods

Decellularization methods, such as sodium dodecyl sulfate (SDS) and Tris-trypsin-triton, are critical for preparing dECM scaffolds, each with distinct advantages and limitations. SDS, a chemical detergent, effectively removes cellular components but can disrupt ECM structure, reducing glycosaminoglycans

(GAGs) and collagen density, leading to increased porosity and decreased mechanical stiffness (25). This may compromise scaffold integrity and cellular interactions. In contrast, Tris-trypsin-triton, combining enzymatic and milder detergent approaches, better preserves ECM components, including GAGs and collagen fibrils, supporting enhanced cell proliferation and infiltration, as seen in MCF-7 cultures (25). However, it requires longer processing times and optimization to ensure complete cell removal. The choice of method depends on the desired scaffold properties, with Tris-trypsin-triton preferred for maintaining native ECM cues and SDS for rapid decellularization despite potential ECM loss (12).

2. METHOD

This systematic review adhered to PRISMA guidelines to evaluate dECM scaffolds in BC and PCa research (26). We searched PubMed, Scopus, and Web of Science (January 2010-June 2025) using terms like "decellularized extracellular matrix," "breast cancer," "prostate cancer," and "tumor microenvironment," supplemented by reference list searches. Inclusion criteria covered peer-reviewed English articles on *in vitro*, *in vivo*, or *ex vivo* dECM studies in BC/PCa. Non-peer-reviewed, irrelevant, or non-English studies were excluded. After deduplication, titles/abstracts were screened, followed by full-text review. The selection process is shown in Fig. 1.

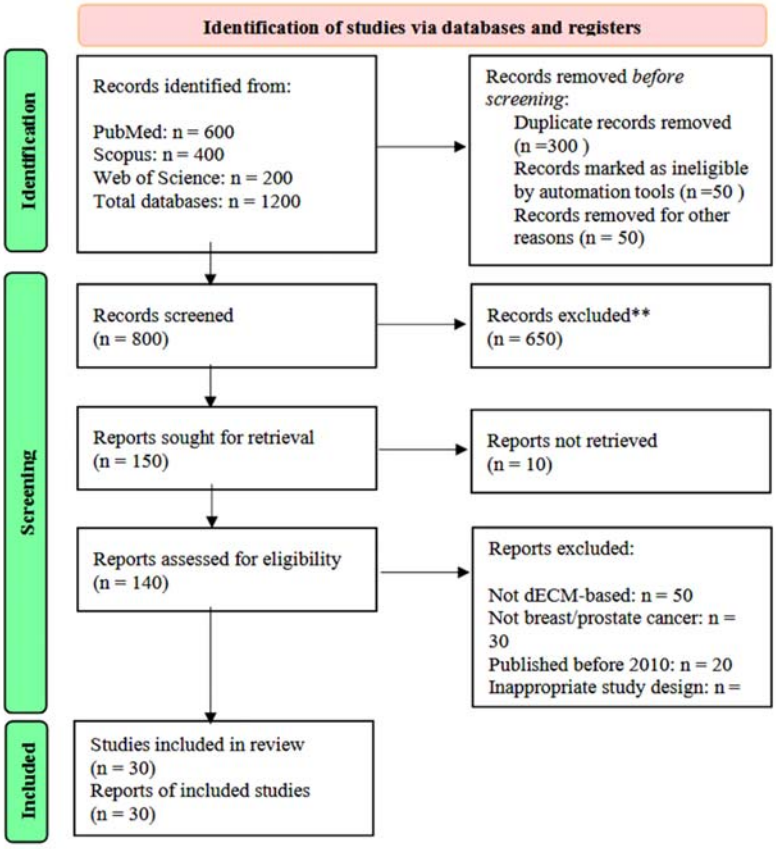

Fig. 1. PRISMA flow diagram illustrating the study selection process for the systematic review of dECM scaffolds in breast and prostate cancer research, covering publications from January 1, 2010, to June 28, 2025. dECM, Decellularized extracellular matrix.

dECM scaffolds, derived from healthy and cancerous breast tissues, provide advanced platforms for culturing breast and other cancer cells. These scaffolds, including decellularized normal and tumor-derived breast tissue, facilitate the study of cellular behavior within biologically relevant systems (Table 1). For instance, Leiva *et al*. (16) utilized a patient-derived scaffold (PDS) from BC samples to investigate alterations in the TME of MCF-7 cells following chemotherapy. Their study revealed that these cells exhibited increased resistance to chemotherapeutic agents, including doxorubicin and 5-fluorouracil (5-Fu). By varying drug types and concentrations, the researchers observed distinct changes in the expression of markers associated with cell proliferation (MKI67, CCNA2), EMT (VIM, SNAI1), and the cancer stem cell (CSC) phenotype (NANOG, POU5F1, CD44, ABCG2), highlighting the utility of dECM scaffolds in elucidating chemotherapy-induced changes in BC cells. Zhu and coworkers (19) developed mammary tissue-derived extracellular matrix hydrogels to assess the effects of radiation therapy-induced ECM changes on BC cell behavior, demonstrating that irradiated dECM hydrogels enhance the proliferation and invasive ability of encapsulated triple-negative BC (TNBC) cells. These effects are driven by alterations in ECM composition, including increased levels of collagens I, IV, VI, and fibronectin, which trigger elevated cytokine secretion within the irradiated microenvironment. This cytokine release promotes an immunosuppressive TME, upregulating invasion-related gene expression and enhancing TNBC aggressiveness (19,27). These findings underscore the role of radiation-induced ECM biochemical changes in modulating TNBC cell behavior, though further studies are needed to fully elucidate specific cytokine-ECM interactions.

Table 1. dECM scaffolds usage in BC tissue engineering.

dECM Source	Decellularization Method	Cell cultured on dECM	Study type	Results	Ref.
Primary BC tissue	Combined chemical (SDS, Triton X-100) and enzymatic (DNase & RNase)	MDA-MB-231, MCF-7 and T-47D cells	*In vitro*	-Increased cancer stem cell features and chemoresistance. -Decreased proliferation.	(16)
Normal lung tissue	Combined chemical (SDS, Triton X-100) and enzymatic (DNase & RNase)	MCF-7 cells	*In vitro*	-Excellent cell compatibility, increased cell growth and proliferation, and expression of BRCA1 and HER2 in MCF-7 cells. -Increased chemoresistance	(24)
TNBC cell-derived tumor-bearing and obese mammary glands	Combined chemical (SDS, Triton X-100) and enzymatic (DNase & RNase)	MDA-MB-231, MDA-MB-468 and MCF-10A cells	*In vitro*/ Mice *in vivo*	-Collagen VI contributes to TNBC cell invasion via NG2-EGFR cross-talk and MAPK signaling.	(18)
Fibroblasts (NIH-3T3 cells and cancer-associated murine fibroblasts)	Combined chemical (SDS, Triton X-100) and enzymatic (DNase & RNase)	MDA-MB-231, MCF-7, and MCF-10A cells	*In vitro*/ Mice *in vivo*	-Activated PI3K-Akt signaling via integrin 1. Changed morphology and cell migration behaviors	(28)
Benign and cancerous breast tumors from cell culture	Enzymatic with trypsin and mild detergents (Triton X-100)	MDA-MB-231, MCF-7, and MCF-10A cells	*In vitro*	-Promoted proliferation of invasive MDA-MB-231 cell-derived dECM -Suppressed proliferation on benign MCF-10A cell-derived dECM. -Increased chemoresistance on invasive MDA-MB-231 cell-derived dECM	(29)
Normal and cancerous lung and liver tissue	Combined chemical (SDS, Triton X-100) and enzymatic (DNase & RNase)	LM2-4 and 4T1 cells	*In vitro*/ Mice *in vivo*	-Promoted cell adhesion and colonization in cancer tissue-derived dECM.	(30)
Healthy breast tissue	Tris-trypsin-triton, an enzymatic and mild detergent-based	KTB-21 and MDA-MB-231 cells	*In vitro*	-Increase in cell migration and invasion in the mice that were exposed to a high-fat diet.	(31)

Table 1. dECM scaffolds usage in BC tissue engineering.

dECM Source	Decellularization Method	Cell cultured on dECM	Study type	Results	Ref.
Lung tissue	Combined chemical (SDS, Triton X-100) and enzymatic (DNase & RNase)	MCF-7 cell	*In vitro*	-Promoted aggressive cell proliferation and viability.	(32)
Bone mimetic dECM from osteoblasts (BM-ECM) Osteosarcoma cells (OS-ECM)	Combined chemical (SDS, Triton X-100) and enzymatic (DNase & RNase)	4T1, MDA-MB-231, MCF-7, and HCC1937 cells	*In vitro*/ mice *in vivo*	-Highly metastatic breast cancer cells tended to adhere and migrate on BM-ECM, while lowly metastatic breast cancer cells preferred the OS-ECM niche.	(33)
Healthy breast tissue TNBC cell	Combined chemical (SDS, Triton X-100) and enzymatic (DNase &RNase)	TNBC and MCF-7 cells	*In vitro*	-ECM from triple-negative BC promoted EMT and reduced the treatment sensitivity of MCF-7 cells.	(34)
MCF-7 cell	Enzymatic with trypsin and mild detergents	MCF-7 cell	*In vitro*	-Showed that autologous CD-dECM can replace hydrogels in tumor organoid generation and culture at low and high concentrations, respectively.	(35)
Irradiated and non-irradiated breast tissue	Combined chemical (SDS, Triton X-100) and enzymatic (DNase & RNase)	MDA-MB-231 and 4T1 cells	*In vitro*/*in vivo* mice	-Radiation-damaged sites promoted TNBC invasion and proliferation as well as an immunosuppressive microenvironment.	(19)
Mouse organ-derived extracellular matrices	Combined chemical (SDS, Triton X-100) and enzymatic (DNase & RNase)	MDA-MB-231 and SKBR-3 cells	*In vitro*/ *in vivo* mice	-Revealed that the larger the ECM mean pore size and the smaller the total stiffness (as in lung and ovary), the more proliferative and invasive the mesenchymal cells became.	(36)
Normal lung tissue	Chemical (SDS, Triton X-100)	MDA-MB-231, MCF-7 and 4T1 cells	*In vitro*	-MDA-MB-231 and 4T1 cells that have undergone EMT can proliferate. -MCF-7 cells that have not undergone EMT died by apoptosis -Knockdown of ZEB1 significantly reduced the invasion and colonization of MDA-MB-231 cells in the decellularized lung	(37)
Normal adipose tissue	Enzymatic with trypsin and mild detergents	MCF-7, BT474, SKBR3 cells	*In vitro*	-Proliferation, underwent EMT, and increased invasion. -Increased chemoresistance via Akt. more sensitive to lapatinib	(38)
Cancerous mammary gland	Combined chemical (SLES) and enzymatic (DNase)	MCF-7 cells	*In vitro*	-Underwent EMT, increased stem cell marker expression, cell migration, proliferation, and chemoresistance.	(39)
A549-derived lung cancer	Combined chemical (SDS, Triton X-100) and enzymatic (DNase & RNase)	MCF-7 cells	*In vitro*/ Mice *in vivo*	-Cell proliferation. -Increased IL-8, bFGF, and VEGF production	(25)
Normal and cancerous breast tissue	Combined chemical (SLES) and enzymatic (DNase)	MCF-7 cells	*In vitro*	-Suppressed proliferation, EMT and angiogenic gene expression, and increased apoptosis in normal tissue-derived dECM. -Promoted MMP-9 production, proliferation, EMT, and angiogenic gene expression and suppressed apoptosis in cancer tissue-derived dECM	(17)
Primary BC tissue	Combined chemical (SDS, Triton X-100) and enzymatic (DNase)	MDA-MB-231 and MCF-7	*In vitro*/ Mice *in vivo*	Underwent EMT, increased stem cell marker expression and cell proliferation	(40)
Amnion membrane	Combined chemical (SDS) and enzymatic (DNase & RNase)	MDA-MB-231 cells	*In vitro*	-Increased cell migration and proliferation. Higher CSC content. -Much more resistant to apoptosis	(41)

BC, Breast cancer; dECM, decellularized extracellular matrix; TNBC, *Triple-Negative breast cancer*; EMT, *epithelial-mesenchymal transition*; SLES, *sodium lauryl ether sulfate*.

Liu *et al*. (39) developed a method to decellularize human BC biopsy samples using a 0.5% sodium lauryl ether sulfate (SLES) solution, creating an *in vitro* model to study BC pathogenesis. Their findings demonstrated that recellularized scaffolds enhanced MCF-7 cell drug resistance, evidenced by reduced apoptosis during 5-Fu treatment, and increased stemness, marked by elevated expression of stem cell markers (Oct4, SOX2) and BC stem cell marker (CD49F).

Additionally, studies have shown that 3D cancer-derived ECM promotes EMT and cancer cell proliferation, while normal breast tissue-derived ECM suppresses EMT and cell growth, instead promoting apoptosis (17). These changes affected differentiation, EMT, stemness, and proliferation. Another study showed that cell-free PDSs derived from primary BC infiltrated with standardized BC cell lines triggered specific changes in cancer cells. These changes affected differentiation, EMT, stemness, and proliferation (40). To assess the effects of individual protein components of the ECM on tumor progression, Wishart *et al*. (18) utilized dECM scaffolds derived from mammary glands of obese and tumor-bearing mice, demonstrating that these scaffolds enhance TNBC invasion by upregulating collagen VI expression, which activates the EGFR/MAPK signaling pathway through NG2-EGFR crosstalk. This interaction promotes the expression of invasion-related genes, thereby facilitating TNBC cell invasiveness. These findings elucidate the mechanistic role of collagen VI in modulating ECM-driven signaling cascades that enhance tumor aggressiveness, providing a clearer understanding of the biochemical cues within the TME.

In a study, Amens and coworkers (31) studied multigenerational obesity's effect on epithelial cell migration and invasion using decellularized breast tissues from mouse pups in a diet-induced obesity model. MDA-MB-231 cancer cells showed increased motility and invasion on matrices from mice with high-fat diet-fed mothers. The study identified increased collagen curvature within the ECM of obese mice as a critical biomechanical factor promoting cancer cell migration and invasion, suggesting that obesity-induced ECM remodeling enhances tumor aggressiveness through altered matrix architecture.

In order to demonstrate the decellularization of other tissues, such as lung, liver, bone, fat, and amniotic membrane for BC research, some studies are presented here. Li *et al*. (24) developed a decellularized porcine lung scaffold to examine BC cell proliferation and drug resistance. MCF-7 cells in this scaffold showed increased proliferation and resistance to 5-Fu, driven by its TME-like features, including porous alveoli-bronchiole architecture, collagen fibers, and hypoxic conditions. The scaffold's large surface area aided cell adhesion, while native collagen fibers enhanced cell-ECM interactions, promoting tumor-like behavior.

Similarly, Xiong *et al.* (37) investigated the colonization of BC cells with varying metastatic potentials within the lung ECM, revealing that lung microvasculature induces dormancy in metastatic cells, while lung fibroblasts promote their proliferation. They demonstrated that decellularized lung tissue retains essential biophysical and biochemical cues, creating a physiologically relevant microenvironment that supports BC cell invasion and colonization.

Lü et al. (25) showed that tumor sheets decellularized by Tris-trypsin-triton multi-step or SDS treatment achieved full cellular removal. However, this process resulted in some loss of ECM components, increased porosity, and reduced mechanical stiffness. Between the two methods, Tris-trypsin-triton was found to be superior to SDS in preserving the structures and components of the ECM, thereby supporting optimal 3D proliferation and repopulation of tumor cells, while also promoting significant secretion of IL-8 (Fig. 2A). Additionally, histological analysis with hematoxylin and eosin (H&E) staining showed that MCF-7 cells in Tris-trypsin-triton-treated scaffolds exhibited greater cell numbers and deeper infiltration at 7, 10, and 13 days compared to SDS-treated scaffolds (Fig. 2B).

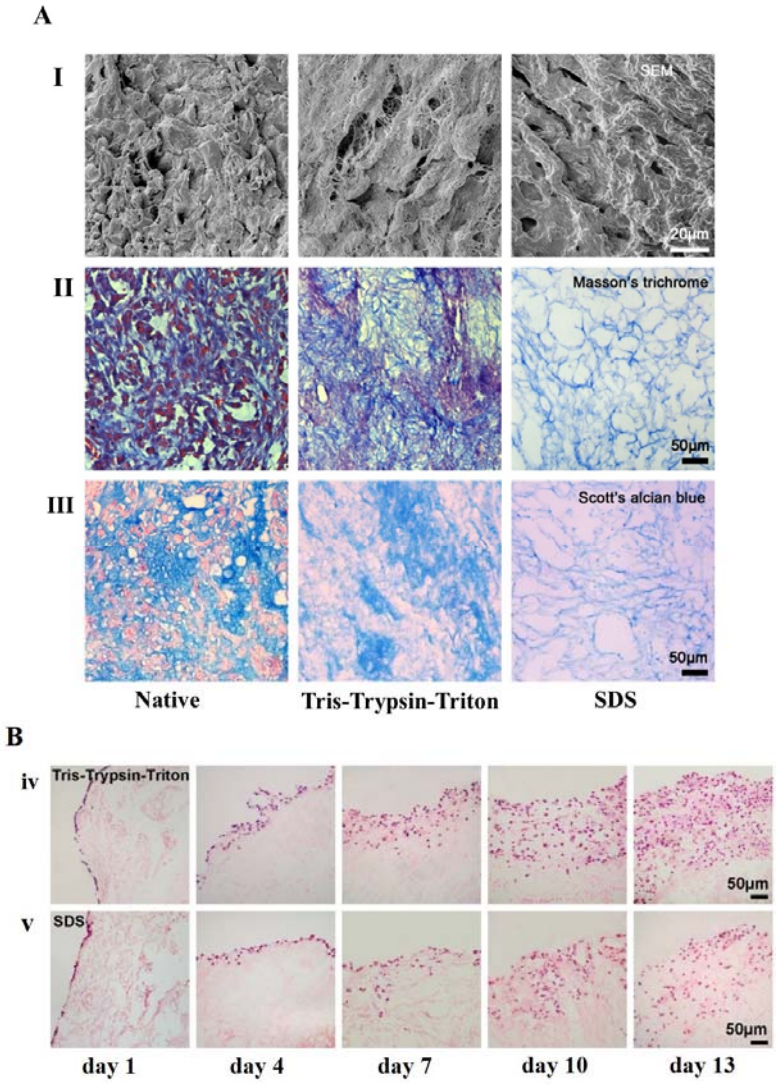

Fig. 2. (A) ECM structure and component investigation of native, Tris-trypsin-triton-treated, and SDS-treated tumor sheets. (I) Scanning electron microscopy (SEM) examination for Tris-trypsin-triton-treated and SDS-treated samples showed a lack of cellular components and more open spaces than the native samples. (II) Collagen fibril stained by Masson's trichrome showing similar distribution of collagen fibrils for Tris-trypsin-triton treated samples, but more sparse distribution of collagen fibrils for SDS-treated samples compared with the native samples. (III) GAG staining with Scott's alcian blue presents mostly retention of GAGs for Tris-trypsin-triton-treated sheets but less GAGs for SDS-treated sheets compared with their native counterparts. (B) H&E-stained histological cross-sections of MCF-7 cells repopulated in the two acellular scaffolds over time. (iv) MCF-7 cells cultured in the Tris-trypsin-triton group, showing an increase in cell numbers and infiltration depths over time. (v) MCF-7 cells cultured in the SDS group, showing fewer cell numbers and infiltration depths compared with the Tris-trypsin-triton treated scaffolds at 7-, 10-, and 13-day culture (Reproduced with permission from reference (25)). ECM, Extracellular matrix; SDS, sodium dodecyl sulfate; GAG, glycosaminoglycan; H&E, hematoxylin and eosin.

Aguado *et al.* (30) revealed that BC cell lines 4T1 and LM2-4 exhibited enhanced adhesion and colonization on dECMs from cancerous liver and lung tissues compared to healthy tissues. The authors suggested that myeloperoxidase plays a role in enhancing cancer cell colonization. The findings of this study support the "seed and soil" hypothesis, which is challenging to explore using traditional biological techniques and materials. In a complementary approach, Wang *et al.* (32) developed a 3D composite scaffold combining decellularized lung ECM with chondroitin sulfate, gelatin, and chitosan to model lung metastasis. This scaffold, mimicking lung matrix properties (stiffness, pore size, alveolar structure), promoted MCF-7 cell pseudopodia formation and reduced

migration compared to porcine decellularized lung matrix. While Aguado *et al.* (30) emphasize biochemical cues (myeloperoxidase) in cancer-altered ECM, Wang *et al.* (32) focus on the biomechanical properties of engineered scaffolds, together providing insights into ECM-driven mechanisms of BC metastasis.

Dunne *et al.* (38) explored the utility of decellularized human adipose tissue (hDAM) as a 3D scaffold for culturing BC cell lines, leveraging its structural similarity to breast tissue. Their results demonstrated that MCF-7 and BT474 cells cultured in hDAM scaffolds exhibited growth patterns more akin to xenografts than to cells cultured on 2D surfaces (Fig. 3). Notably, these cells displayed increased resistance to doxorubicin, suggesting that the 3D microenvironment may enhance chemoresistance. Additionally, SKBR3 and BT474 cells in hDAM scaffolds showed elevated EGFR and AKT phosphorylation, correlating with heightened sensitivity to lapatinib, indicating that 3D scaffolds may modulate signaling pathways differently than 2D cultures. Ganjibakhsh *et al.* (41) investigated the behavior of BC cells cultured on decellularized amnion membrane (DAM) scaffolds compared to 2D cultures. They established NaOCl treatment as an effective decellularization method to generate a natural 3D scaffold (Fig. 4A). BC cells in DAM scaffolds exhibited greater resistance to apoptosis following cisplatin treatment, alongside upregulated expression of stemness markers OCT3/4 and SOX2 after a four-day drug-free culture period, compared to 2D cultures (Fig. 4B). Pospelov *et al.* (36) further elucidated the role of biomechanical properties in decellularized scaffolds, demonstrating that matrix characteristics significantly influence cancer cell behavior. Mesenchymal phenotype cells, such as MDA-MB-231, preferentially proliferated in matrices with reduced stiffness and larger pore sizes, while epithelial phenotype cells, such as SKBR-3, required softer local stiffness at the fiber scale to support growth, underscoring the importance of scaffold biomechanics in cell-specific responses.

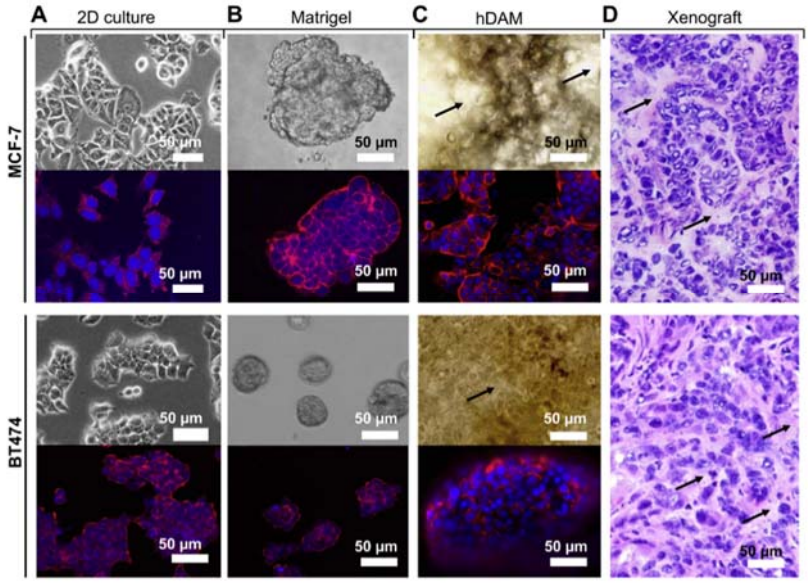

Fig. 3. Cellular organization of breast cancer cells in 2D cultures, Matrigel, hDAM, and xenografts. MCF-7 and BT474 cells cultured using (A) 2D surfaces, (B) Matrigel, and (C) hDAM scaffolds were examined by phase contrast microscopy and fluorescence confocal microscopy. Cells were stained with rhodamine-conjugated phalloidin (red; binds F-actin) and DAPI (blue). (D) Tissue slides from xenografts were processed with H&E staining and examined by bright-field microscopy to visualize the cellular organization of tumor sections. 2D-cultured MCF-7 and BT474 cells formed monolayers. When cultured on Matrigel, MCF-7 and BT474 cells formed distinct 3D spheroids. MCF-7 and BT474 cells cultured in hDAM scaffolds formed a large number of spherical cell aggregates that occupied the porous space within the nanofibrous scaffolds. These cellular aggregates were interconnected within scaffolds and resembled the xenografts in cell organization. The ECM in hDAM and tumor slides is indicated by black arrows (Reproduced with permission from reference (38)). hDAM, Human adipose tissue-derived extracellular matrix; H&E, hematoxylin and eosin.

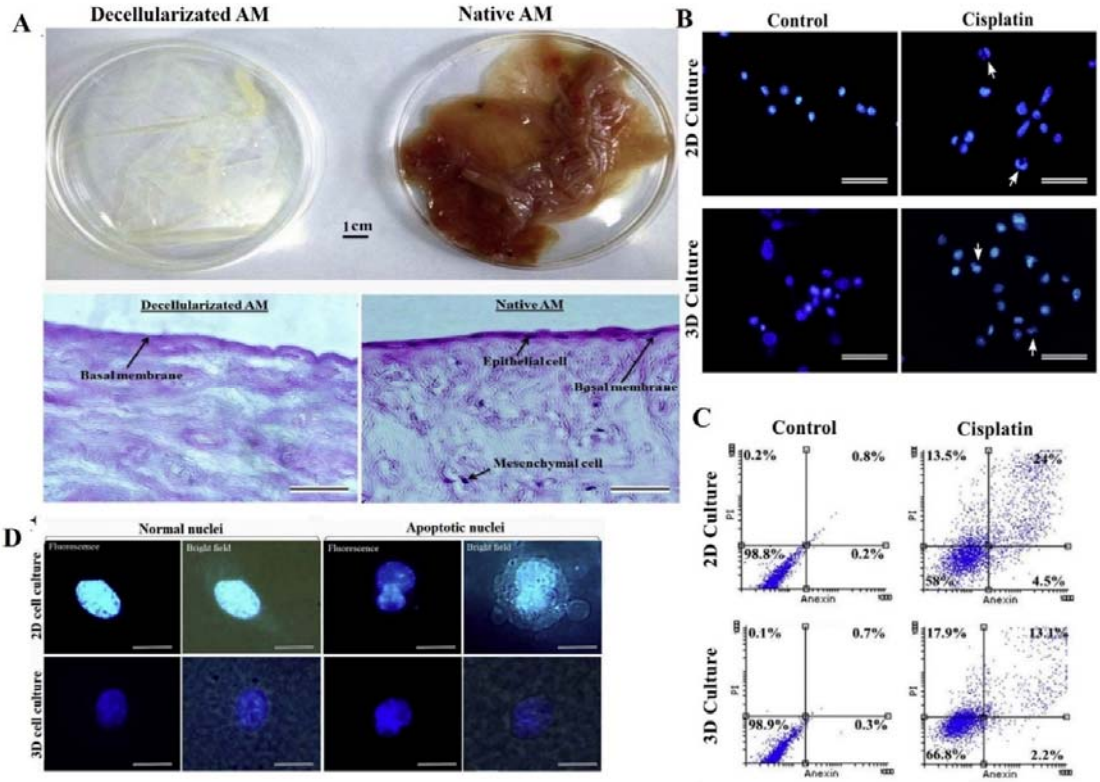

Fig. 4. Histological analysis of the DAM scaffold. (A) The apparent difference between the native AM and DAM scaffold is due to the removal of cells from the membrane. As shown in the H&E-stained cross-section of native AM and DAM scaffold, complete removal of cells in the DAM scaffold was confirmed (Scale bar: 50 μm). (B) Apoptotic morphological assessment by Hoechst 33258 staining (B, Scale bar: 50 μm). The cisplatin-treated cells exhibit fragmented nuclei (arrow), whereas in the control, a normal morphology of nuclei was observed. (C) Flow cytometry analysis of Annexin-V and propidium iodide (PI) staining of apoptotic cells following cisplatin treatment (59 μM for 48 h) in 2D culture and 3D DAM scaffolds. Annexin V positive cells (right-down) indicate the percentage of early apoptotic cells, and the Annexin V and PI double positive cells (right-up) indicate the percentage of late apoptotic cells. (D) High magnification of normal and apoptotic nuclei in both 2D and 3D models (F, Scale bar: 50 μm). (Reproduced with permission from the reference (41)). DAM, Decellularized amnion membrane; AM, amnion membrane; H&E, hematoxylin and eosin.

Collectively, these studies emphasize the value of 3D decellularized scaffolds as physiologically relevant platforms for studying tumor behavior and developing targeted therapies, with biomechanical properties serving as critical determinants of cellular outcomes.

The aforementioned study utilized dECM sourced from either healthy or cancerous tissues. However, the other source of dECM is the use of tissue generated by cell culture. For this purpose, Castelló and colleagues (28) developed a 3D dECM from both normal NIH-3T3 fibroblasts and cancer-associated fibroblasts, due to their high ECM production. They examined the behavior of MCF-7, MDA-MB-231, and benign MCF-10A breast cell lines in these scaffolds. MCF-10A cells adopted a spindle-like morphology, MCF-7 cells maintained a rounded, less spread shape, and MDA-MB-231 cells exhibited enhanced spindle shapes in dECM derived from cancer-associated fibroblasts, associated with Akt pathway activation, indicating that the ECM source influences cell morphology and signaling (Fig. 5).

Hoshiba *et al.* (29) found that ECM derived from normal mammary gland cells inhibited BC cell proliferation, whereas ECM from MDA-MB-231 cells promoted MDA-MB-231 and MCF-7 cell growth. MCF-10A cells were unaffected by cancer-derived ECM but showed stimulated proliferation on MCF-10A-derived ECM. Additionally, the chemoresistance of MDA-MB-231 cells to 5-Fu increased when exposed to ECM from the same cancer cells. These results suggest that cellular responses vary depending on the ECM's origin, reflecting different stages of tumorigenesis and cell malignancy.

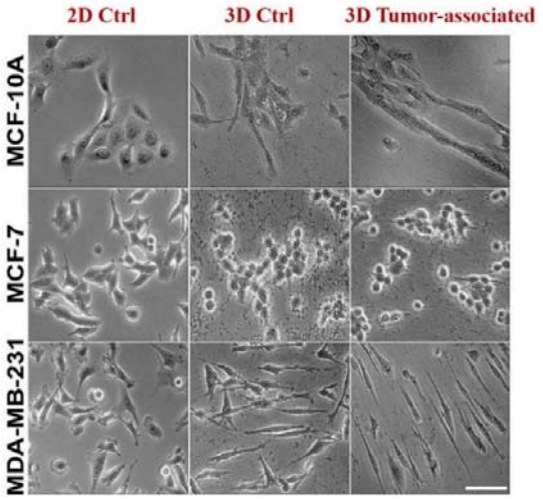

Fig. 5. Phase contrast transmitted light micrographs depicting changes in cell morphologies of the various cell lines in response to the 2D and 3D substrates are shown; the scale bar represents 75 µm (Reproduced with permission from reference (28)).

A study revealed that ECM derived from triple-negative BC (TN-ECM) created an estrogen receptor-negative and highly metastatic environment for BC cells. This occurs by decreasing estrogen receptor alpha (ERα) expression, enhancing cell proliferation, and triggering EMT in ER-positive MCF-7 cells, which may facilitate BC metastasis (34). In research, dECMs derived from MCF-7 cells were produced and subsequently transformed into autologous hydrogels that are biologically active, biocompatible, and non-immunogenic. These hydrogels were intended to serve as a microenvironment for both organoid formation and culture (35).

Weng *et al.* (33) identified two distinct cellular microenvironments: the bone mimetic niche (BM-ECM) and the bone tumor mimetic niche (OS-ECM). BM-ECM, with higher collagen and GAGs content, outperformed OS-ECM and COLI in detecting early metastatic BC cells in a nude mouse model, highlighting its potential for early metastasis detection.

In a comprehensive synthesis of the conducted studies, 3D ECM-based scaffolds serve as physiologically relevant models, demonstrating enhanced chemoresistance, altered signaling pathways, and phenotype-specific responses in BC cells, thereby advancing tumor biology research and personalized therapeutic development. The origin and biomechanical properties of ECM critically regulate malignancy, metastasis, and drug response, establishing robust platforms for preclinical investigations.

3. PCaCELL BEHAVIORS IN/ON dECM

PCa relapse, primarily caused by the metastasis of cancer cells, significantly contributes to the high mortality rate among patients. This highlights the increasing demand for effective tumor models to investigate PCa metastasis (42). dECM scaffolds provide 3D platforms to study PCa cell behaviors, such as adhesion, proliferation, migration, and chemoresistance, as detailed in Table 2.

Table 2. dECM scaffolds usage in PCa tissue engineering.

dECM Source	Decellularization Method	Cell cultured on dECM	Study type	Results	Ref.
hBM-MSCs	Combined chemical (SDS, Triton X-100) and enzymatic (DNase)	PCa-LNCaP, PCa cells (PC3), and MDA-PCa-2b	*In vitro*	-Promoted cancer cell proliferation and docetaxel resistance -Increased the phosphorylation of MAPK pathway-related proteins	(43)
Human primary osteoblast	Combined chemical (SDS, Triton X-100) and enzymatic (DNase)	LNCaP, PC3	*In vitro*	-Increased cell adhesion, proliferation, invasive potential, Ca^{2+} signaling, and osteolysis.	(44)
Spinach leaves	Combined chemical (SDS, Triton X-100) and enzymatic (DNase)	PC3 and SK-MEL-28	*In vitro*	-Increased sensitivity to radiation and drug treatment -Downregulated YAP/TAZ signaling pathway -Decreased cell proliferation	(45)

Table 2. dECM scaffolds usage in PCa tissue engineering.

dECM Source	Decellularization Method	Cell cultured on dECM	Study type	Results	Ref.
Fibroblast and osteoblast	Combined chemical (SDS, Triton X-100) and enzymatic (DNase)	PC3, DU145, and VCaP cells	*In vitro*	-Endo180 is upregulated in metastatic prostate cancer cells in contact with human ECM -Endo180 cooperates with fibroblast-derived LOX to promote metastatic prostate cancer cell migration	(46)
Human normal and cancerous Prostate tissue	Combined chemical (SDS, Triton X-100) and enzymatic (DNase)	RWPE-1, BPH.1, and PC3 cells	*Ex vivo/ in vitro*	-Non-tumoral samples showed a uniform, dense network of well-intersected fibers. -Tumor samples showed fused and well-separated filaments.	(47)
Natural, BPH, and malignant human prostate tissues	Combined chemical (SDS, Triton X-100) and enzymatic (DNase & RNase)	PC-3, LNCaP, and prostate stromal cells	*In vitro/ in vivo*: rat	The cancerous rat model demonstrated the highest decrease in the ECM content after recellularization.	(48)

dECM, Decellularized extracellular matrix; PCa, prostate cancer.

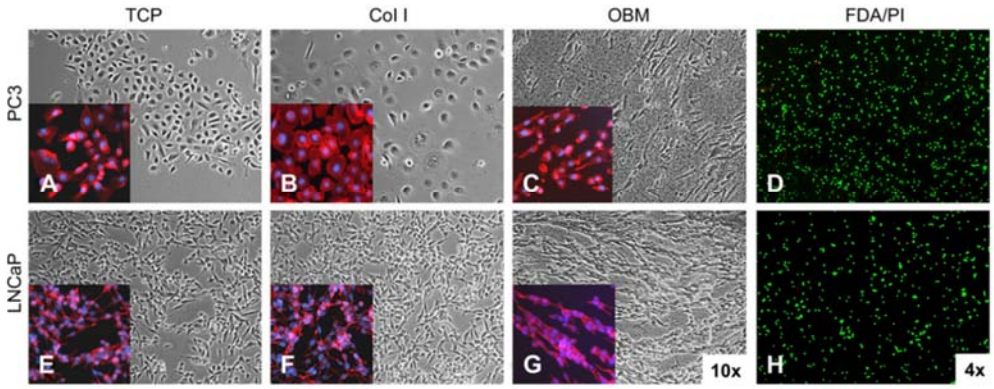

Fig. 6. After 48 h of culture on OBM, PC3 displayed an altered morphology compared to the epithelial morphology observed on TCP or collagen I coating (A, B, C), assuming an elongated, fibroblast-like, spindle-shaped phenotype (C) as demonstrated in the light microscopy images (magnification 10×) and Phalloidin/DAPI staining (insets, magnification10×). PC3 cell viability on OBM was assessed at > 95% (D, magnification 4×). After 5 days, similar changes were observed in LNCaP, also assuming a linear arrangement within the bone matrix, aligning themselves with the fibrillar structure of the matrix (G). FDA/PI staining showed a viability of > 95% for LNCaPs (H) (Reproduced with permission from reference (44)). TCP, tissue culture polystyrene; OBM, osteoblast-derived matrix; FDA/PI, fluorescein diacetate / propidium iodide; Col I, collagen I.

To better understand the spread of PCa cells to the bone marrow microenvironment, Lescarbeau *et al*. (43) stated that bone marrow-derived ECM enhanced LNCaP survival, promoted androgen-independent growth, and increased docetaxel resistance, underscoring ECM's role in modulating PCa behavior and chemoresistance. Cazzaniga *et al*. (47) developed an *ex vivo/in vitro* model by decellularizing prostate specimens from radical prostatectomy and co-culturing them with primary PCa cells to assess invasiveness. After cell removal, non-tumoral samples showed a uniform, dense network of consistently sized fibers, while malignant samples exhibited a looser structure with intertwined filaments forming distinct, well-separated chords that influence cancer cell behavior. The research group of Reichert *et al*. (44) utilized decellularized matrix from primary human osteoblasts to study PCa behavior in the bone microenvironment. LNCaP and PCa cells (PC3) cultured on this matrix showed strong adhesion and increased proliferation, along with changes in their phenotypes. PC3 transformed into an elongated, fibroblast-like shape, while LNCaP arranged linearly in alignment with the matrix's fibrillar structure (Fig. 6).

A study found that ECM from human osteoblasts and fibroblasts facilitated a rounded, amoeboid-like migration and increased Endo180 expression in three PCa cell lines. The interaction between Endo180 and the rigid microenvironment, mediated by lysyl oxidase (LOX), was identified as a potential target for reducing metastatic progression in PCa (46). Kajbafzadeh *et al.* (48) examined the ECM composition in the prostate tissue. Their histological analyses after decellularization revealed decreased expression of laminin and vimentin in normal, benign prostatic hyperplasia (BPH), and malignant tissues. Notably, malignant samples had significantly lower levels of type IV collagen in the ECM. Post-implantation immunostaining of the recellularized scaffolds revealed no cancerous cells during follow-up, suggesting effective decellularization.

Plant tissues can be decellularized to produce cellulose scaffolds that support both cell lines and primary cells for *in vitro* culture. This process has gained significant interest recently as a sustainable method for creating scaffolds that can be repopulated with human cells (45). A study found that PC3 and melanoma cells (SK-MEL-28) were more sensitive to radiation and drug treatments when cultured on decellularized spinach leaf scaffolds compared to traditional rigid cell culture platforms, associated with a downregulation of YAP/TAZ signaling, due to lower substrate stiffness. Cells displayed altered morphology, reduced proliferation, and a rounded shape with diffuse F-actin distribution, contrasting with the polygonal shape and prominent F-actin stress fibers on plastic substrates (Fig. 7) (45).

Contradictions in dECM studies for BC and PCa arise from variations in ECM source, decellularization methods, and tumor context, with some studies indicating that dECM from normal breast tissue suppresses EMT and proliferation of BC cells (17), while tumor-derived dECM promotes EMT, stemness, and invasion (39,34). These discrepancies are compounded by differences in ECM stiffness, where primary tumors exhibit moderate stiffness (1-5 kPa) due to collagen deposition, while metastases display higher stiffness (10–20 kPa) driven by enhanced collagen crosslinking and LOX activity, correlating with denser collagen networks and increased aggressiveness in both BC and PCa metastases. Standardization of dECM protocols and comparative studies is essential to resolve these inconsistencies and elucidate the role of ECM stiffness in tumor progression (49,50).

4. CONCLUDING REMARKS AND FUTURE PERSPECTIVES

dECM scaffolds have emerged as a powerful tool in BC and PCa research, effectively recapitulating the native TME by preserving tissue-specific architecture and biochemical cues, thus enabling detailed studies of tumor behavior and therapeutic responses. In BC, patient- or tumor-derived dECM promotes EMT, stemness, and chemoresistance, particularly in TNBC, enhancing invasion and proliferation. Conversely, PCa dECM, often derived from bone marrow, reflects metastatic bone tropism by increasing adhesion, proliferation, and docetaxel resistance, highlighting disease-specific microenvironmental influences. However, challenges persist, including variability in dECM composition due to patient-specific differences and disease states, which complicates standardization and reproducibility. Decellularization techniques, such as chemical or enzymatic methods, may degrade critical ECM components like collagen or GAGs, compromising scaffold bioactivity and fidelity in mimicking the TME. Additionally, the heterogeneous nature of cancer limits model generalizability, as dECM from specific tissues may not fully capture diverse TME dynamics, and low yields from cell-derived matrices compared to tissue sources hinder scalability, necessitating advanced bioengineering solutions.

To overcome these limitations, standardizing decellularization protocols and employing advanced analytical tools, such as mass spectrometry, can ensure consistent scaffold quality. Integrating dECM with organoids or microfluidic systems can also better model immune-tumor and stromal interactions, thereby enhancing physiological relevance. Emerging bioengineering approaches, including 3D bioprinting and nanomaterial integration, allow precise control over scaffold architecture, enabling tailored models that replicate the fibrous TME of BC or the bone-like matrix of metastatic PCa. Incorporating growth factors, cytokines, and signaling molecules into dECM further enhances its ability to reflect cancer

heterogeneity, while artificial intelligence (AI) facilitates analysis of complex proteomic and structural data to identify cancer-specific biomarkers, such as those associated with PCa metastasis. Hybrid models combining dECM with organ-on-chip platforms enable dynamic studies of tumor behavior, drug response, and metastasis, addressing the scarcity of clinical data for therapeutic validation. Advances in bioreactor technology can optimize cell-derived matrices yield, improving scalability, while novel decellularization methods that preserve ECM integrity enhance scaffold functionality for personalized cancer modeling. By addressing variability, scalability, and clinical translation challenges through interdisciplinary collaboration, dECM scaffolds hold immense potential to advance TME simulation, inform regenerative medicine, and develop targeted therapies for improved patient outcomes in BC and PCa.

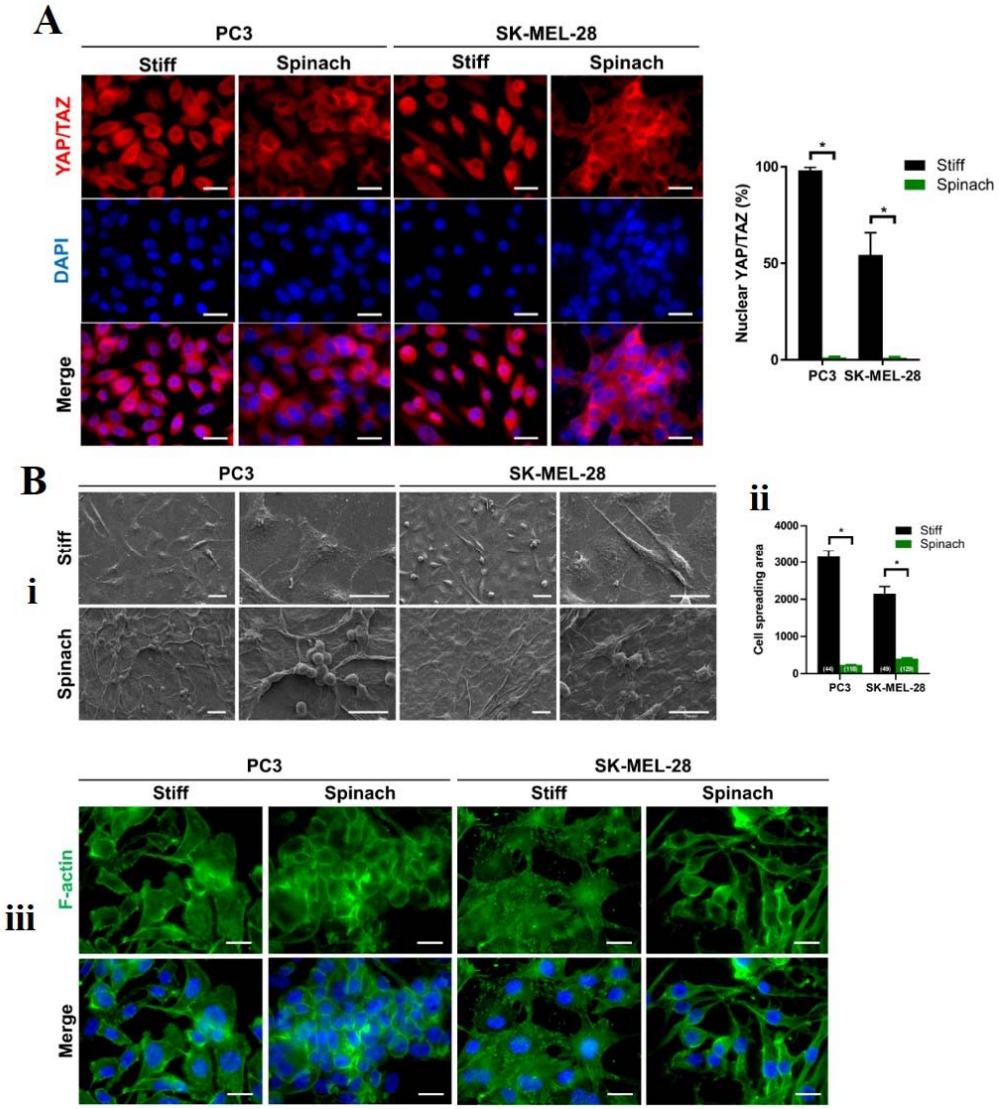

Fig. 7. (A) Immunofluorescence images of YAP/TAZ and nuclei (DAPI) in PC3 and SK-MEL-28 cells seeded on a coverslip and spinach scaffold for 3 days. Scale bars = 15 μm. Graphs indicate the percentage of cells with nuclear YAP/TAZ (n = 3, **P* < 0.05; Student t-test). (B) Cell culture on a leaf scaffold induced cell morphology changes. (i) Representative SEM images of PC3 and SK-MEL-28 cells cultured on a stiff substrate (coverslip) or spinach leaf scaffold for 3 days. The cell images were collected in three independent experiments (n = 3). Scale bars = 20 μm. (ii) Histogram showing the changes of cell spreading area on stiff and leaf substrates and represented as mean ± SEM (n = 3, **P* < 0.05; Mann-Whitney test). The numbers shown in parentheses indicate cell numbers for statistics of the cell spreading area examined in each case. (iii) Immunofluorescence images of F-actin and nuclei (DAPI) in PC3 and SK-MEL-28 cells seeded on a stiff substrate (coverslip) and spinach scaffold. Scale bars = 15 μm (Reproduced with permission from reference (45)). SEM, Scanning electron microscope.

5. ADDITIONAL INFORMATION

Acknowledgments

This research did not receive any specific grant from funding agencies in the public, commercial, or not-for-profit sectors.

Conflict of interest statement

All authors declare that there are no financial/commercial conflicts of interest.

Authors' contributions

Sh. Ghaedamini conducted the primary investigation, created visualizations, provided essential resources, and drafted the initial manuscript. Z. Sadeghi, F. Rahmani, and M. Anjomshoa contributed to the investigation and reviewed and edited the manuscript. A. Honarvar conceptualized the study, managed project administration, and revised the manuscript. All authors have read and approved the finalized article. Each author has fulfilled the authorship criteria.

6. REFERENCES

1. Shoari A, Khodabakhsh F, Ahangari Cohan R, Salimian M, Karami E. Anti-angiogenic peptides application in cancer therapy;a review. Res Pharm Sci. 2021;16(6):559-574. DOI: 10.4103/1735-5362.327503.
2. Costard LS, Hosn RR, Ramanayake H, O'Brien FJ, Curtin CM. Influences of the 3D microenvironment on cancer cell behaviour and treatment responsiveness: a recent update on lung, breast and prostate cancer models. Acta Biomater. 2021;132:360-378. DOI: 10.1016/j.actbio.2021.01.023.
3. Ghaedamini Sl, Hashemibeni B, Honarvar A, Rabiei A, Karbasi S. Recent innovations in strategies for breast cancer therapy by electrospun scaffolds:a review. J Polym Environ. 2023;32(3):1-27. DOI: 10.1007/s10924-023-03022-6.
4. Ghaedamini Sl, Kazemi M, Rabiei A, Honarvar A, Aliakbari M, Karbasi S. Anti-tumor effects of ellagic acid and mesenchymal stem cell-conditioned medium on breast cancer cells on the 3D printed PCL/agarose scaffolds. J Drug Deliv Sci Tech. 2024;101(10):106315. DOI: 10.1016/j.jddst.2024.106315.
5. Hoshiba T. Decellularized extracellular matrix for cancer research. Materials. 2019;12(8):1311,1-16. DOI: 10.3390/ma12081311.
6. Negishi J, Yamaguchi A, Tanaka D, Hashimoto Y, Zhang Y, Funamoto S. A method for fabricating tissue-specific extracellular matrix blocks from decellularized tissue powders. Adv Biol (Weinh). 2025;9(1):e2400398. DOI: 10.1002/adbi.202400398.
7. Gholami K, Izadi M, Heshmat R, Aghamir SMK. Exploring the potential of solid and liquid amniotic membrane biomaterial in 3D models for prostate cancer research:a comparative analysis with 2D models. Tissue Cell. 2025;93:102726. DOI: 10.1016/j.tice.2025.102726.
8. Zhang L, Zhou J, Kong W. Extracellular matrix in vascular homeostasis and disease. Nat Rev Cardiol. 2025;22(5):333-353. DOI: 10.1038/s41569-024-01103-0.
9. Ferreira LP, Gaspar VM, Mano JF. Decellularized extracellular matrix for bioengineering physiomimetic 3d *in vitro* tumor models. Trends Biotechnol. 2020;38(12):1397-1414. DOI: 10.1016/j.tibtech.2020.04.006.
10. Pierantoni L, Silva-Correia J, Motta A, Reis RL, Oliveira JM. Biomaterials as ECM-like matrices for 3D *in vitro* tumor models. Biomaterials for 3D Tumor Modeling. Elsevier. 2020;157-173. DOI: 10.1016/B978-0-12-818128-7.00007-1.
11. Bonnans C, Chou J, Werb Z. Remodelling the extracellular matrix in development and disease. Nat Rev Mol Cell Biol. 2014;15(12):786-801. DOI: 10.1038/nrm3904.
12. Yao Q, Zheng YW, Lan QH, Kou L, Xu HL, Zhao YZ. Recent development and biomedical applications of decellularized extracellular matrix biomaterials. Mater Sci Eng C Mater Biol Appl. 2019;104:109942,1-10. DOI: 10.1016/j.msec.2019.109942.
13. Tian X, Werner ME, Roche KC, Hanson AD, Foote HP, Yu SK, *et al*. Organ-specific metastases obtained by culturing colorectal cancer cells on tissue-specific decellularized scaffolds. Nat Biomed Eng. 2018;2(6):443-452. DOI: 10.1038/s41551-018-0231-0.
14. Alabi BR, LaRanger R, Shay JW. Decellularized mice colons as models to study the contribution of the extracellular matrix to cell behavior and colon cancer progression. Acta Biomater. 2019;100:213-222. DOI: 10.1016/j.actbio.2019.09.033.
15. Guo X, Liu B, Zhang Y, Cheong S, Xu T, Lu F, et al. Decellularized extracellular matrix for organoid and engineered organ culture. J Tissue Eng. 2024;(15):20417314241300386. DOI: 10.1177/20417314241300386.
16. Leiva MC, Garre E, Gustafsson A, Svanström A, Bogestål Y, Håkansson J, *et al*. Breast cancer patient-derived scaffolds as a tool to monitor chemotherapy responses in human tumor microenvironments. J Cell Physiol. 2021;236(6):4709-4724. DOI: 10.1002/jcp.30191.
17. Jin Q, Liu G, Li S, Yuan H, Yun Z, Zhang W, *et al*. Decellularized breast matrix as bioactive microenvironment for *in vitro* three-dimensional cancer culture. J Cell Physiol. 2019;234(4):3425-3435. DOI: 10.1002/jcp.26782.

18. Wishart AL, Conner SJ, Guarin JR, Fatherree JP, Peng Y, McGinn RA, *et al*. Decellularized extracellular matrix scaffolds identify full-length collagen VI as a driver of breast cancer cell invasion in obesity and metastasis. Sci Adv. 2020;6(43):1-13. DOI: 10.1126/sciadv.abc3175.
19. Zhu T, Alves SM, Adamo A, Wen X, Corn KC, Shostak A, *et al*. Mammary tissue-derived extracellular matrix hydrogels reveal the role of irradiation in driving a pro-tumor and immunosuppressive microenvironment. Biomaterials. 2024;308:122531,1-29. DOI: 10.1016/j.biomaterials.2024.122531.
20. Micek HM, Visetsouk MR, Masters KS, Kreeger PK. Engineering the extracellular matrix to model the evolving tumor microenvironment. iScience. 2020;23(11):101742,1-12. DOI: 10.1016/j.isci.2020.101742.
21. Kort-Mascort J, Bao G, Elkashty O, Flores-Torres S, Munguia-Lopez JG, Jiang T, *et al*. Decellularized extracellular matrix composite hydrogel bioinks for the development of 3d bioprinted head and neck *in vitro* tumor models. ACS Biomater Sci Eng. 2021;7(11):5288-5300. DOI: 10.1021/acsbiomaterials.1c00812.
22. Romero-López M, Trinh AL, Sobrino A, Hatch MM, Keating MT, Fimbres C, *et al*. Recapitulating the human tumor microenvironment:colon tumor-derived extracellular matrix promotes angiogenesis and tumor cell growth. Biomaterials. 2017;116:118-129. DOI: 10.1016/j.biomaterials.2016.11.034.
23. Koh I, Cha J, Park J, Choi J, Kang SG, Kim P. The mode and dynamics of glioblastoma cell invasion into a decellularized tissue-derived extracellular matrix-based three-dimensional tumor model. Sci Rep. 2018;8(1):4608,1=12. DOI: 10.1038/s41598-018-22681-3.
24. Li W, Hu X, Yang S, Wang S, Zhang C, Wang H, *et al*. A novel tissue-engineered 3D tumor model for anti-cancer drug discovery. Biofabrication. 2018;11(1):015004,1-35. DOI: 10.1088/1758-5090/aae270.
25. Lü WD, Zhang L, Wu CL, Liu ZG, Lei GY, Liu J, *et al*. Development of an acellular tumor extracellular matrix as a three-dimensional scaffold for tumor engineering. PLoS One. 2014;9(7):e103672,1-13. DOI: 10.1371/journal.pone.0103672.
26. Page MJ, McKenzie JE, Bossuyt PM, Boutron I, Hoffmann TC, Mulrow CD, *et al*. The PRISMA 2020 statement: an updated guideline for reporting systematic reviews. BMJ. 2021;372:n71,1-9. DOI: 10.1136/bmj.n71.
27. Guo S, Yao Y, Tang Y, Xin Z, Wu D, Ni C, *et al*. Radiation-induced tumor immune microenvironments and potential targets for combination therapy. Signal Transduct Target Ther. 2023;8(1):205,1-22. DOI: 10.1038/s41392-023-01462-z.
28. Castelló-Cros R, Khan DR, Simons J, Valianou M, Cukierman E. Staged stromal extracellular 3D matrices differentially regulate breast cancer cell responses through PI3K and beta1-integrins. BMC Cancer. 2009;9:94,1-19. DOI: 10.1186/1471-2407-9-94.
29. Hoshiba T, Tanaka M. Breast cancer cell behaviors on staged tumorigenesis-mimicking matrices derived from tumor cells at various malignant stages. Biochem Biophys Res Commun. 2013;439(2):291-296. DOI: 10.1016/j.bbrc.2013.08.038.
30. Aguado BA, Caffe JR, Nanavati D, Rao SS, Bushnell GG, Azarin SM, *et al*. Extracellular matrix mediators of metastatic cell colonization characterized using scaffold mimics of the pre-metastatic niche. Acta Biomater. 2016;33:13-24. DOI: 10.1016/j.actbio.2016.01.043.
31. Amens JN, Bahçecioğlu G, Dwyer K, Yue XS, Stack MS, Hilliard TS, *et al*. Maternal obesity driven changes in collagen linearity of breast extracellular matrix induces invasive mammary epithelial cell phenotype. Biomaterials. 2023;297:122110,1-20.
32. Wang L, Yang J, Hu X, Wang S, Wang Y, Sun T, *et al*. A decellularized lung extracellular matrix/chondroitin sulfate/gelatin/chitosan-based 3D culture system shapes breast cancer lung metastasis. Biomater Adv. 2023;152:213500. DOI: 10.1016/j.bioadv.2023.213500.
33. Weng B, Li M, Zhu W, Peng J, Mao X, Zheng Y, *et al*. Distinguished biomimetic dECM system facilitates early detection of metastatic breast cancer cells. Bioeng Transl Med. 2023;9(1):e10597,1-19. DOI: 10.1002/btm2.10597.
34. Tan Q, Xu L, Zhang J, Ning L, Jiang Y, He T, *et al*. Breast cancer cells interact with tumor-derived extracellular matrix in a molecular subtype-specific manner. Biomater Adv. 2023;146:213301,1-11. DOI: 10.1016/j.bioadv.2023.213301.
35. Tevlek A. The role of decellularized cell derived extracellular matrix in the establishment and culture of *in vitro* breast cancer tumor model. Biomed Mater. 2024;19(2). DOI: 10.1088/1748-605X/ad2378.
36. Pospelov AD, Kutova OM, Efremov YM, Nekrasova AA, Trushina DB, Gefter SD, *et al*. Breast cancer cell type and biomechanical properties of decellularized mouse organs drives tumor cell colonization. Cells. 2023;12(16):1-26. DOI: 10.3390/cells12162030.
37. Xiong G, Flynn TJ, Chen J, Trinkle C, Xu R. Development of an *ex vivo* breast cancer lung colonization model utilizing a decellularized lung matrix. Integr Biol (Camb). 2015;7(12):1518-1525. DOI: 10.1039/c5ib00157a.
38. Dunne LW, Huang Z, Meng W, Fan X, Zhang N, Zhang Q, *et al*. Human decellularized adipose tissue scaffold as a model for breast cancer cell growth and drug treatments. Biomaterials. 2014;35(18):4940-4949. DOI: 10.1016/j.biomaterials.2014.03.003.
39. Liu G, Wang B, Li S, Jin Q, Dai Y. Human breast cancer decellularized scaffolds promote epithelial-to-mesenchymal transitions and stemness of breast cancer cells *in vitro*. J Cell Physiol. 2019;234(6):9447-9456. DOI: 10.1002/jcp.27630.

40. Landberg G, Fitzpatrick P, Isakson P, Jonasson E, Karlsson J, Larsson E, *et al*. Patient-derived scaffolds uncover breast cancer promoting properties of the microenvironment. Biomaterials. 2020;235:119705,1-15.
DOI: 10.1016/j.biomaterials.2019.119705.
41. Ganjibakhsh M, Mehraein F, Koruji M, Aflatoonian R, Farzaneh P. Three-dimensional decellularized amnion membrane scaffold as a novel tool for cancer research;cell behavior, drug resistance and cancer stem cell content. Mater Sci Eng C Mater Biol Appl. 2019;100:330-340.
DOI: 10.1016/j.msec.2019.02.090.
42. Demirkaya D. Development of a hydrogel based prostate tumor model for cancer cell migration studies:Middle East Technical University; 2022:1-83.
43. Lescarbeau RM, Seib FP, Prewitz M, Werner C, Kaplan DL. *In vitro* model of metastasis to bone marrow mediates prostate cancer castration resistant growth through paracrine and extracellular matrix factors. PLoS One. 2012;7(8):e40372,1-11.
DOI: 10.1371/journal.pone.0040372.
44. Reichert JC, Quent VM, Burke LJ, Stansfield SH, Clements JA, Hutmacher DW. Mineralized human primary osteoblast matrices as a model system to analyse interactions of prostate cancer cells with the bone microenvironment. Biomaterials. 2010;31(31):7928-7936.
DOI: 10.1016/j.biomaterials.2010.06.055.
45. Lacombe J, Harris AF, Zenhausern R, Karsunsky S, Zenhausern F. Plant-based scaffolds modify cellular response to drug and radiation exposure compared to standard cell culture models. Front Bioeng Biotechnol. 2020;8:932,1-15.
DOI: 10.3389/fbioe.2020.00932.
46. Caley MP, King H, Shah N, Wang K, Rodriguez-Teja M, Gronau JH, *et al*. Tumor-associated Endo180 requires stromal-derived LOX to promote metastatic prostate cancer cell migration on human ECM surfaces. Clin Exp Metastasis. 2016;33(2):151-165.
DOI: 10.1007/s10585-015-9765-7.
47. Cazzaniga W, Nebuloni M, Longhi E, Locatelli I, Allevi R, Lucianò R, *et al*. Human prostate tissue-derived extracellular matrix as a model of prostate microenvironment. Eur Urol Focus. 2016;2(4):400-408.
DOI: 10.1016/j.euf.2016.02.016.
48. Kajbafzadeh AM, Jafarnezhad-Ansariha F, Sharifi SHH, Sabetkish S, Parvin M, Tabatabaei S, *et al*. Decellularization and recellularization of natural, benign prostatic hyperplasia and malignant human prostatic tissues:role of extracellular matrix behavior on development of prostate cancer. Regen Eng Transl Med. 2023;9(1):533-546.
DOI: 10.1007/s40883-023-00299-w.
49. Tamayo-Angorrilla M, López de Andrés J, Jiménez G, Marchal JA. The biomimetic extracellular matrix: a therapeutic tool for breast cancer research. Transl Res. 2022;247:117-136.
DOI: 10.1016/j.trsl.2021.11.008.
50. Lv Y, Wang H, Li G, Zhao B. Three-dimensional decellularized tumor extracellular matrices with different stiffness as bioengineered tumor scaffolds. Bioact Mater. 2021;6(9):2767-2782.
DOI: /10.1016/j.bioactmat.2021.02.004.